Hindawi
Adsorption Science & Technology
Volume 2023, Article ID 8532316, 17 pages
https://doi.org/10.1155/2023/8532316

Research Article

Recovering the Soybean Hulls after Peroxidase Extraction and Their Application as Adsorbent for Metal Ions and Dyes

Aleksandra Ivanovska,[1] **Biljana Dojčinović**,[2] **Jelena Lađarević**,[3] **Leposava Pavun**,[4] **Dušan Mijin**,[3] **Mirjana Kostić**,[3] **and Milica Svetozarević**[1]

[1]*University of Belgrade, Innovation Center of the Faculty of Technology and Metallurgy, 11000 Belgrade, Serbia*
[2]*University of Belgrade, Institute of Chemistry, Technology and Metallurgy, 11000 Belgrade, Serbia*
[3]*University of Belgrade, Faculty of Technology and Metallurgy, 11000 Belgrade, Serbia*
[4]*University of Belgrade, Faculty of Pharmacy, 11000 Belgrade, Serbia*

Correspondence should be addressed to Aleksandra Ivanovska; aivanovska@tmf.bg.ac.rs

Received 24 October 2022; Revised 19 December 2022; Accepted 4 February 2023; Published 22 February 2023

Academic Editor: Monoj Kumar Mondal

This study is aimed at extending the soybean hulls' lifetime by their utilization as an adsorbent for metal ions (Cd^{2+} and Cu^{2+}) and dyes (Reactive Yellow 39 (RY 39) and Acid Blue 225 (AB 225)). ATR-FTIR spectroscopy, FE-SEM microscopy, and zeta potential measurements were used for adsorbent characterization. The effect of the solution's pH, peroxidase extraction, adsorbent particle size, contact time, the pollutant's initial concentration, and temperature on the soybean hulls' adsorption potential was studied. Before peroxidase extraction, soybean hulls were capable of removing 72% Cd^{2+}, 71% Cu^{2+} (at a pH of 5.00) or 81% RY 39, and 73% AB 225 (at a pH of 3.00). For further experiments, soybean hulls without peroxidase were used for several reasons: (1) due to their observed higher metal ion removal, (2) in order to reduce the waste disposal cost after the peroxidase (usually used for wastewater decolorization) extraction, and (3) since the soybean hulls without peroxidase possessed significantly lower secondary pollution than those with peroxidase. Cd^{2+} and Cu^{2+} removal was slightly increased when the smaller adsorbent fraction (710-1000 μm) was used, while the adsorbent particle size did not have an impact on dye removal. After 30 min of contact time, 92% and 88% of RY 39 and AB 225 were removed, respectively, while after the same contact time, 80% and 69% of Cd^{2+} and Cu^{2+} were removed, respectively. Adsorption of all tested pollutants follows a pseudo-second-order reaction through the fast adsorption, intraparticle diffusion, and final equilibrium stage. The maximal adsorption capacities determined by the Langmuir model were 21.10, 20.54, 16.54, and 17.23 mg/g for Cd^{2+}, Cu^{2+}, RY 39, and AB 225, respectively. Calculated thermodynamic parameters suggested that the adsorption of all pollutants is spontaneous and of endothermic character. Moreover, different binary mixtures were prepared, and the competitive adsorptions revealed that the soybean hulls are the most efficient adsorbent for the mixture of AB 225 and Cu^{2+}. The findings of this study contribute to the soybean hulls' recovery after the peroxidase extraction and bring them into the circular economy concept.

1. Introduction

Water quality represents one of the major concerns of the twenty-first century, and therefore, surface and deep-water pollution is a topic of high social and scientific interest in both developing and already developed countries. It is well known that water pollution is closely related to various anthropogenic activities (such as mining, dyeing, municipal and industrial solid waste disposal, incineration and/or openly burning waste, and agricultural soil fertilization [1]), unplanned urbanization, and rapid industrialization. Among many inorganic and organic pollutants, heavy metals and dyes receive widespread attention; their presence in wastewater is a major problem since most of them are potentially hazardous to the environment and human health. Namely, heavy metals are toxic, nondegradable, carcinogenic, and persistent; they enter our body system through the ingestion of food and water and air [2]. The relationship between environmental exposure

to heavy metals and various human diseases was recently investigated by Đukić-Ćosić et al. [3], Baralić et al. [4], Buha et al. [5], and many other researchers all over the world. On the other hand, dyes are complex organic pollutants mainly present in textile, cosmetic, paper, leather, rubber, and printing industries' wastewaters. Their presence in wastewater even at small concentrations aggravates photosynthesis; dyes disable the sun rays' adsorption in surface waters and negatively affect the surrounding flora and fauna [6]. Not only is the suppression of aquatic biota growth and reproduction caused by these pollutants [6] but also excessive exposure to dye degradation products causes skin irritation as well as respiratory problems [7]. In response to the rising demands for clean and safe water, many different technologies are utilized for the purification of metal and/or dye contaminated wastewater [8]. Some of them include membrane separation, chemical and electrochemical technologies, reverse osmosis, ion exchange, electrodialysis, electrolysis, and adsorption procedures. Excluding adsorption, all of them require substantial financial input, high energy consumption, altogether restricting their utilization for wastewater treatment. On the other hand, adsorption using conventional and nonconventional adsorbents is an easy-handled and environmentally acceptable method for various pollutants' removal. It enables adsorbents' regeneration and operation under a broad range of process settings and has better selectivity [2]. Since magnetic nanocomposites have a large specific surface area, they were recently used as adsorbents for metals and dyes [9–12]. Compared to conventional adsorbents (*i.e.*, activated carbons, ion-exchange resins, and inorganic materials such as alumina, silica gel, and zeolites), green waste-derived adsorbents are economically viable (their cost-potential makes them competitive) and have proven satisfactory adsorption capacities toward heavy metals and dyes. The most studied green waste-derived adsorbents are sugar beet shreds [13], fibers [14–17], rice husk [18], wood-based adsorbents [2, 19–21], potato peels [22, 23], and other cellulose-based adsorbents [7]. Although green waste-derived materials are intensively studied as adsorbents for heavy metal ions and dyes, the exploration of new eco-friendly, biodegradable, low-cost, and abundant adsorbents that have low/no negative impact on the environment remains primary focus of investigation among researchers.

The rapid world soybean (*Glycine max* L.) production (about 385 million metric tons in 2021-2022, SOPA) and utilization worldwide result in the intensive generation of soybean processing waste—hulls that are rich in soybean peroxidase. We decided to extend the soybean hulls' lifetime and utilize them as adsorbents for metal ions and dyes since this processing waste is easily available and can be used without additional treatments (or after the peroxidase extraction in water). Moreover, soybean hulls have a myriad of functional groups (COOH, OH, *etc.*) which are capable of binding metals and dyes, while their porous structure contributes to a high ability to swell and store a high amount of solution. First, the used adsorbent was characterized in terms of its surface morphology (assessed by FE-SEM), chemistry (using ATR-FTIR), and electrokinetic properties (*i.e.*, zeta potential). The influence of various parameters such as peroxidase extraction, solution pH, adsorbent particle size, contact time, the pollutant's initial concentration, and temperature on the soybean hulls' adsorption potential for cadmium or copper ions as well as textile dyes Reactive Yellow 39 (RY 39) or Acid Blue 225 (AB 225) (their structures are given in the Supplementary material, see Figures S1a and S2a) was investigated. Many reasons are behind the selection of these four pollutants. Namely, the World Health Organization (WHO) has identified cadmium as one of ten chemicals of major public health concern [24]. The connection between long-term exposure to this toxic metal and various renal syndromes, osteoporosis and osteomalacia, endocrine-disrupting properties, and different types of cancer has already been established [25–27]. Copper is an essential nutrient for humans, animals, and plants; however, its toxicity is a much overlooked contributor to many health problems including anorexia, migraine headaches, allergies, childhood hyperactivity, and learning disorders [28]. Furthermore, RY 39 and AB 225 were not selected randomly; contrary to many other dyes, their structures are not significantly influenced by the pH change (see Figures S1c and S2c). This enables us to eliminate the influence of the dyes' structural changes caused by the solution's pH, and therefore, their adsorption can be ascribed solely to the soybean hulls' surface chemistry and morphology. Among different classes of synthetic dyes, azo dyes, like AB 225, are one of the most important synthetic dyes produced worldwide [29]. Their degradation byproducts have a toxic and mutagenic impact on aquatic organisms [16]. Furthermore, the second major synthetic dye class is anthraquinone dyes such as RY 39 which are used for dyeing wool, cotton, silk, and polyamide. Nonetheless, their toxicological profiles state that most anthraquinone dyes are mutagenic, carcinogenic, and allergenic [6].

After the adsorption from the single pollutant solution was investigated, different binary mixtures were prepared and competitive metal ion and dye adsorptions were examined. In order to make a more detailed study, one part of the manuscript is focused on water secondary pollution (*i.e.*, leaching of organic and inorganic matter in the water) during adsorption onto soybean hulls (with and without peroxidase). The results of this investigation offer a novel valorization route, *i.e.*, soybean hulls' recovery after the peroxidase extraction that brings them into the circular economy concept through their utilization as adsorbents for inorganic and organic pollutants. It has to be underlined that the utilization of this kind of adsorbent avoids secondary pollution, *i.e.*, the leaching of organic and inorganic matter from the adsorbent.

2. Materials and Methods

2.1. Materials. Soybean hulls were obtained from Sojaprotein d.o.o., Bečej, Serbia. The used chemicals were of the highest commercial grades and used as received.

To study the effect of peroxidase extraction on the soybean hulls' adsorption potential towards metal ions and dyes, two types of soybean adsorbents were used separately. Namely, one set of experiments was performed using

soybean hulls as received, *i.e.*, with peroxidase, while the other set of experiments was carried out after peroxidase extraction. The extraction of the enzyme from soybean hulls was achieved according to the procedure described by Svetozarević et al. [30]. The procedure was repeated until the peroxidase has not been detected. Before the adsorption experiments, dry soybean hulls were ground in a mill, whereby their particle sizes were in the range of 710-1000 and 1000-1500 μm, see Figure 1.

2.2. Methods

2.2.1. Soybean Hulls' Characterization. To prove the existence of peroxidase in the sample SH+PO as well as its successful extraction from the SH-PO sample (see Figure 1), the enzyme activity was assessed according to the previously published method [30].

ATR-FTIR spectroscopy (Nicolet™ iS™ 10 FT-IR (Thermo Fisher 2 SCIENTIFIC) spectrometer with Smart iTR™ attenuated total reflectance (ATR) sampling accessory) was used for the evaluation of the SH+PO and SH-PO surface chemistry. The spectra were recorded in the range of 4000-600 cm^{-1} with 32 scans per spectrum. Based on the ATR-FTIR absorbance spectra, the so-called hydrogen bond intensity (HBI), lateral order index (LOI), and cross-linked lignin ratio (CLL) were calculated as ratios of the intensities of the bands at 3338 and 1334 cm^{-1}, 1429 and 897 cm^{-1}, and 1600 and 1508 cm^{-1}, respectively [31].

The adsorbents' zeta potential as a function of pH was determined by a streaming potential method using a SurPASS electrokinetic analyzer (Anton Paar GmbH, Austria) following the procedure given by Ivanovska and Kostić [32].

SH+PO and SH-PO surface morphology was assessed by FESEM (Tescan MIRA 3 XMU). Before the analysis, the samples were sputter-coated with Au/Pd alloy.

2.2.2. Adsorption Experiments from Single-Pollutant Solution. The adsorption of Cd^{2+} or Cu^{2+} has been carried out from a monometallic solution of $CdCl_2{\cdot}2.5H_2O$ or $CuSO_4{\cdot}5H_2O$, while the adsorption of RY 39 or AB 225 was performed from their appropriate single-pollutant aqueous solutions. A 0.25 g of adsorbent was immersed in 100 ml of single-pollutant aqueous solution and constantly shaken. The adsorption optimization took place in two steps:

(1) The optimization of the initial solution pH: $c_0 = 25$ mg/l, $t = 24$ h, $T = 25^{\circ}$C, pH = 3-6 or 2-5 (for metal ions and dyes, respectively), equal portions of both particle sizes; samples SH+PO and SH-PO

(2) The optimization of the adsorbent particle size: $c_0 = 25$ mg/l, $t = 24$ h, $T = 25^{\circ}$C, pH = 5.00 or 3.00 (for metal ions and dyes, respectively), the adsorbent particle size of 710-1000 or 1000-1500 μm; samples SH-PO1 and SH-PO2

The kinetic, isotherm, and thermodynamic experiments were performed on a sample SH-PO1 under the optimized conditions shown in Table 1. The kinetic and equilibrium adsorption data were interpreted according to a set of widely used kinetic and isotherm models, respectively.

Pollutant removal by soybean hulls was calculated based on its residual concentration in the aqueous solution by using Equation (1), while the mass of adsorbed pollutant per gram adsorbent (q, mg/g) was calculated using Equation (2)

$$\text{Pollutant removal}\,(\%) = \frac{c_0 - c_t}{c_0} \cdot 100, \tag{1}$$

$$q\,(\text{mg/g}) = \frac{c_0 - c_t}{m} \cdot V, \tag{2}$$

where c_0 is the initial pollutant concentration in the solution, mg/l; c_t is the pollutant concentration in the solution after a certain time, mg/l; m is the adsorbent mass, g; and V is the solution volume, l.

The thermodynamic parameters: standard Gibbs free energy (ΔG^0), standard enthalpy (ΔH^0), and standard entropy (ΔS^0) were calculated using Equations (3) and (4)

$$\Delta G^0 = -R \bullet T \bullet \ln\left(K_{\text{eq}}\right), \tag{3}$$

$$\Delta G^0 = \Delta H^0 - T \bullet \Delta S^0, \tag{4}$$

where R is the universal gas constant (8.314 J/mol K), T is the process temperature (K), K_{eq} is the process equilibrium constant calculated as the ratio between the amount of adsorbed pollutant q_e (mg/g) and the residual pollutant concentration in the solution C_e (mg/ml) at the equilibrium.

$$K_{\text{eq}} = \frac{q_e}{C_e}. \tag{5}$$

The expression of the equilibrium constant quantifies the distribution of the pollutant between the solution and the adsorbed phase. By combining Equation (3) and (4), Equation (6) was obtained:

$$\ln\left(K_{\text{eq}}\right) = -\frac{\Delta H^0}{RT} + \frac{\Delta S^0}{R}. \tag{6}$$

The K_{eq} and ΔG^0 were calculated for each studied temperature, while the values of ΔH^0 and ΔS^0 were estimated from the slope and intercept of $\ln\left(K_{\text{eq}}\right)$ *vs.* $1/T$ plot, respectively.

All adsorption experiments were performed in triplicate with standard deviations below 2.2%.

Inductively coupled plasma optical emission spectrometry (ICP-OES, iCAP 6500 Duo ICP, Thermo Fisher Scientific, Cambridge, United Kingdom) was used for the determination of metal concentrations at Cd II 226.502 nm and Cu I 324.754 nm emission lines. The dye concentration in the aqueous solution was determined based on the UV-Vis (Shimadzu 1700 spectrophotometer) absorbance spectra at $\lambda_{\max}$ at 390 and 628 nm for RY 39 and AB 225, respectively.

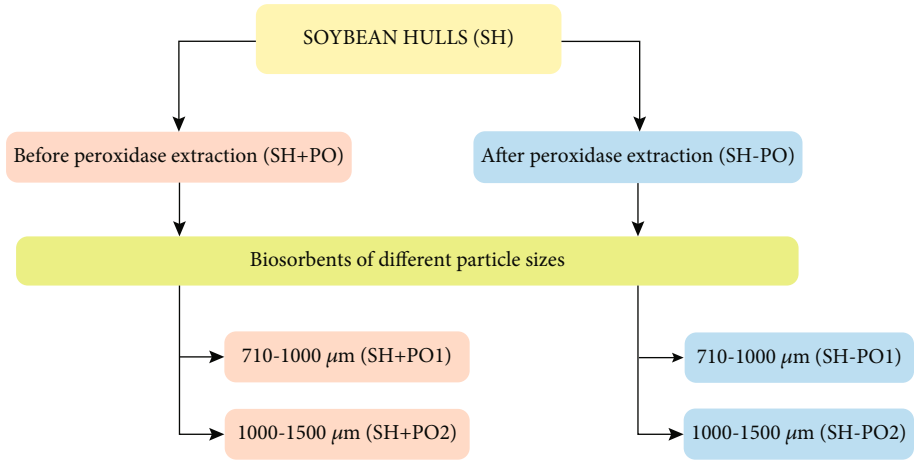

Figure 1: Adsorbents' abbreviations.

Table 1: The kinetic, isotherm, and thermodynamic experiments' conditions.

Experimental conditions	Kinetic experiments		Isotherm experiments		Thermodynamic experiments	
	Metal ions	Dyes	Metal ions	Dyes	Metal ions	Dyes
Initial pollutant concentration	25 mg/l		25-100 mg/l		25 mg/l	
Contact time	420 min		120 min	90 min	120 min	90 min
Temperature	25°C				25, 35, or 45°C	
Solution pH	5.00	3.00	5.00	3.00	5.00	3.00
Particle size	710-1000 μm (sample SH-PO1)					

2.2.3. Competitive Adsorption Experiments. To study the competitive dye and metal ion adsorption, four binary mixtures (RY 39+Cd^{2+}, RY 39+Cu^{2+}, AB 225+Cd^{2+}, and AB 225 +Cu^{2+}) were prepared at pH of 3.00 and 5.00, while the mixtures containing solely dyes and solely metals were prepared at pH of 3.00 and 5.00, respectively. The other experimental conditions were as follows: 25 mg/l initial concentration of each pollutant, contact time of 120 min, and equal portions of both adsorbent particle sizes (sample SH-PO, see Figure 1). The presented results are the average of three measurements in parallel; the standard deviations were below 1.9%.

2.2.4. Study of the Secondary Pollution. The secondary pollution, *i.e.*, leaching of soybean hulls' organic and inorganic matter in the water, was studied by adding 0.25 g of the adsorbents SH+PO and SH-PO in 100 ml of demineralized water at pH of 3.00 (since the metal ion adsorption was carried out at this pH) and constantly shaken for 24 h. Thereafter, the contents of different elements (Al, B, Ba, Ca, Cd, Co, Cu, Cr, Fe, K, Li, Mg, Mn, Na, Ni, Sr, Pb, and Zn) in demineralized water were compared with those determined in the water after the adsorbent's removal. The content of organic matter in the above-mentioned samples was estimated by the dichromate index (chemical oxygen demand (COD)) according to the appropriate standard [33].

3. Results and Discussion

3.1. Characterization of SH Adsorbents. Bearing in mind that the peroxidase removal changes the soybean hull's overall structure, before the evaluation of the SH+PO and SH-PO adsorption potential for metal ions and organic dyes, their characterization was performed. In light of that, the enzyme activity assay was used as a key indicator of peroxidase extraction efficiency. The first extract showed peroxidase activity of 200 U/ml, while after the third cycle of extraction, the peroxidase activity within sample SH-PO was below the level of detection. Furthermore, from the examined samples FE-SEM microphotographs (see Figure 2), it is evident that the soybean hull's surface partially collapses after the enzyme's extraction (SH-PO) being more compressed than before the extraction (SH+PO), which is in accordance with the literature [34]. It is worth mentioning that peroxidase's removal also contributes to a smoother soybean hull surface morphology compared to the rough SH+PO surface with pronounced pores (see Figure 2, sample SH+PO).

Considering the ATR-FTIR spectra of SH+PO and SH-PO (see Figure 3(a)), it could be observed that the peroxidase extraction induces noticeable modifications of the adsorbents' surface chemistry. A spectrum of the SH+PO displays characteristic bands inherent to lignocellulosic materials. Namely, the broad band between 3600 and 3000 cm^{-1} corresponds to mutual O–H and N–H stretching vibrations

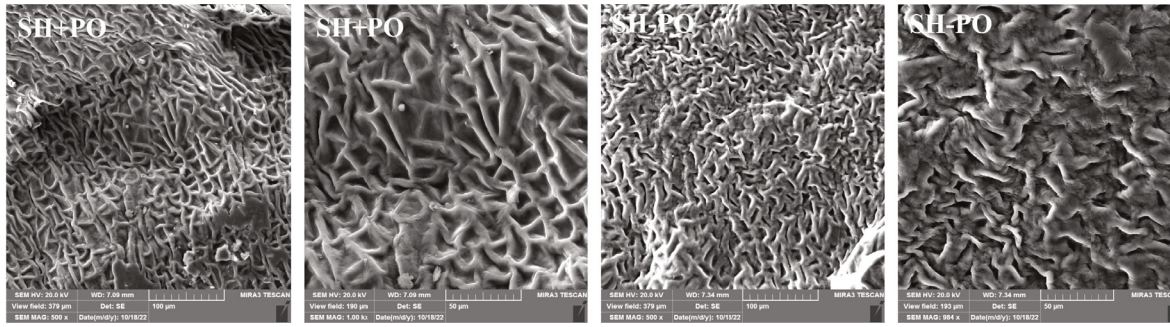

Figure 2: FE-SEM microphotographs of SH+PO and SH-PO (different magnifications).

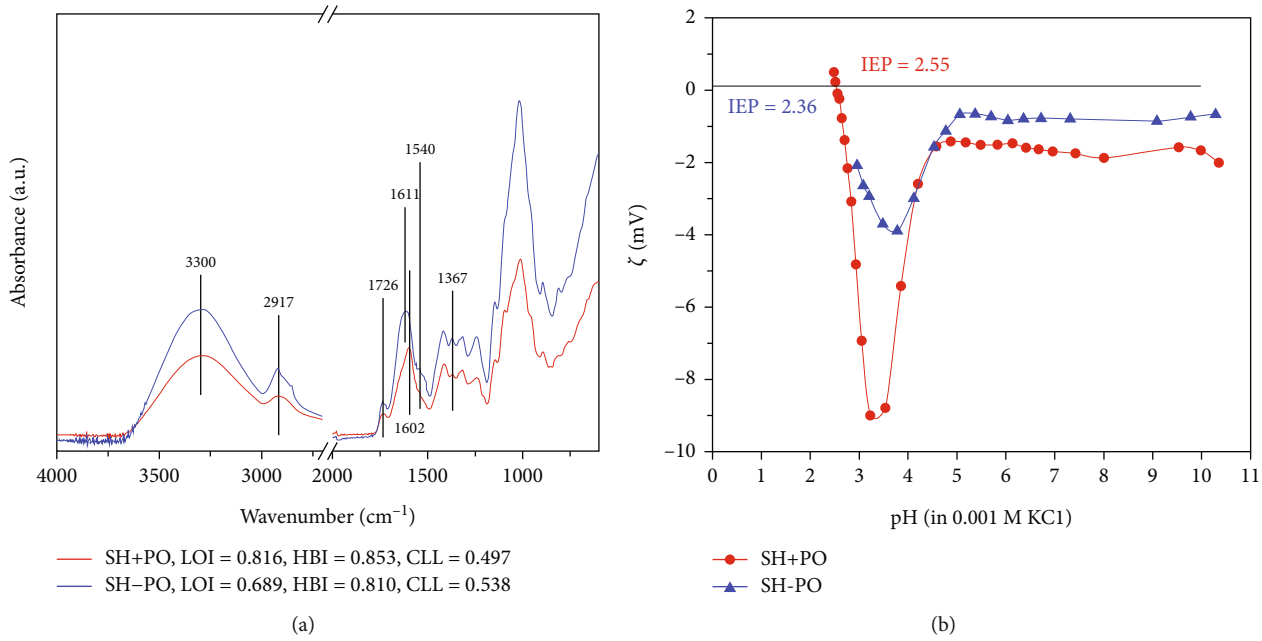

Figure 3: (a) ATR-FTIR spectra and (b) zeta potential (ζ) of the studied soybean hulls.

(related to a peptide-based enzyme), while the band at 2917 cm^{-1} originates from C–H stretching vibrations. A low-intensity band at 1726 cm^{-1} appears from stretching vibrations of characteristic C=O groups. Due to the complexity of the soybean hulls' surface chemistry, a relatively wide band centered at 1602 cm^{-1} could be ascribed to different vibrations ranging from C=O peptide, C=C, and COO^{-} stretching vibrations [35] and absorbed water [34]. After peroxidase extraction, the band at 3300 cm^{-1} becomes intensified, while the band at 2907 cm^{-1} is sharper (see Figure 3(a)). Furthermore, the band at 1602 cm^{-1} observed in the SH+PO spectrum shifts to a higher wavenumber (1611 cm^{-1}) after peroxidase removal. This behavior is followed by a change in its shape and intensity indicating significant changes in the soybean hulls' surface functionality. Moreover, the bands at 1540 and 1367 cm^{-1} related to the lignin backbone become stronger suggesting the enrichment of the lignin content after the extraction of the peptide-based enzyme. Empirical ratios (LOI, HBI, and CLL [31]) calculated from ATR-FTIR spectra could be used to explain the changes that cellulose and lignin moieties (within soybean hulls) underwent enzyme extraction. LOI is closely related to the amount of cellulose crystalline moieties, *i.e.*, represents the ordered regions perpendicular to the chain direction, which is greatly influenced by the chemical processing of cellulose [36], while HBI refers to the degree of the intramolecular hydrogen bond regularity. Upon enzyme extraction, both LOI and HBI values are lowered, indicating a less ordered cellulose structure with lower hydrogen bonding intensity between neighboring cellulose chains and hence lower crystallinity of SH-PO. On the other hand, CLL is related to the amount of lignin with condensed and cross-linked properties. A higher CLL value calculated for SH-PO (0.538) in comparison with that of SH+PO (0.497) could be ascribed to the higher cross-linking and condensation of lignin chains caused by the earlier mentioned soybean hulls' collapse after the enzyme extraction treatment.

The changes in the soybean hulls' surface chemistry after the peroxidase extraction were further proven by the measurement of SH+PO and SH-PO zeta potential. The results presented in Figure 3(b) pointed out that both adsorbents' surfaces are negatively charged at pH values above 2.36

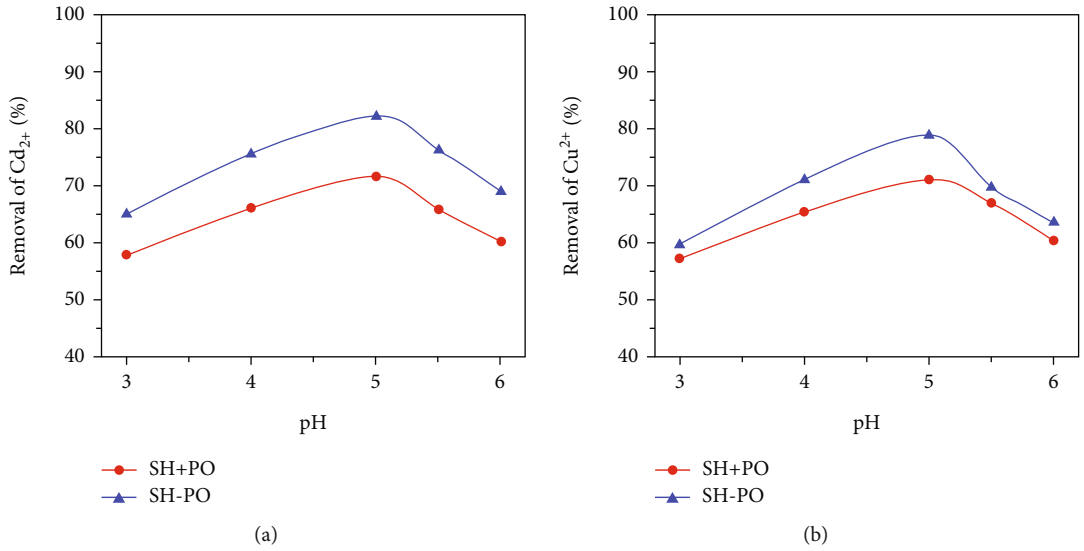

Figure 4: Effect of solution pH on (a) Cd^{2+} and (b) Cu^{2+} removal by soybean hulls.

(SH+PO) and 2.55 (SH-PO), respectively, with the surface of SH-PO being less negative.

3.2. The Influence of Solution pH on the Removal of Metal Ions and Dyes. Among the different adsorption variables, the effect of the solution's initial pH value on pollutant removal was first considered (see Figure 4) since it affects both the solubility and ionization state of the investigated cadmium and copper salts and dyes, as well as the soybean hulls' surface charge [37].

In highly acidic conditions, *i.e.*, at a pH of 3.00, the SH +PO and SH-PO affinity for binding Cd^{2+} and Cu^{2+} is low (removal is ranged between 57 and 65%) due to the excessive H^+ competing with metal ions for the soybean hull surface active sites. As is evident from Figure 4, for both studied adsorbents (SH+PO and SH-PO), maximal heavy metal removals (between 71 and 82%) were achieved at pH 5.00. With a further increase of the solution's pH, a higher concentration of OH^- in the solution leads to the precipitation of Cd^{2+} and Cu^{2+} in the form of hydroxides [38] which hinder the adsorption and thus lower Cd^{2+} and Cu^{2+} removal. Based on the presented results, and in order to achieve maximum Cd^{2+} and Cu^{2+} removal by soybean hulls without incurring precipitation, pH 5.00 was chosen as optimal and used for further experiments. Sanni et al. [39] also found pH 5.00 as optimal for Cu^{2+} removal by citric acid-modified soybean hulls, reaching 40% Cu^{2+} removal, which is much lower than the results obtained in the current study.

Besides the fact that both studied adsorbents behaved similarly regarding the solution's pH, it has to be emphasized that the removal of Cd^{2+} and Cu^{2+} increased after the peroxidase's extraction by 14.6 and 10.9%, respectively. Although zeta potential measurements showed that the SH-PO negative charge is lower than that of SH+PO, its adsorption capacity for the metal ions is surprisingly reinforced. Such differences could be explained by the changes in the soybean hulls' surface physico-chemical properties that occurred after the peroxidase removal. Tummino et al. [34] ascribed the higher adsorption potential of SH-PO to the effect of the intrinsic metal ions present in the enzyme competing with metal ions for adsorbent active sites. Furthermore, the surface chemistry of the soybean hulls is modified after peroxidase extraction in terms of the availability of the groups that are capable and preferential for metal binding. As discussed previously, constituents within the lignocellulosic soybean hulls (primarily cellulose and lignin) are less ordered after peroxidase extraction. For this reason, the functional groups that were responsible for the interactions between these components are no longer constrained and are accessible for the interactions with metal ions.

Taking into account that the adsorption of Cu^{2+} and Cd^{2+} does not correlate with the negative value of the zeta potential, it could be concluded that it is not solely governed by electrostatic interactions with the negatively charged surface. Considering the involvement of different soybean hulls' groups (proven by the ATR-FTIR spectra, Supplementary Material, see Figure S3), it could be suggested that metals are adsorbed onto soybean hulls *via* different binding mechanisms such as surface complexation (involving hydroxyl and carboxyl groups), ion exchange (between adsorbent H^+ and metal ions, also established *via* hydroxyl and carboxyl groups) [40], and cation-π interactions (between the electron-rich phenyl groups of lignin and metal ions) [41] (see Figure 5, displayed for Cu^{2+}, the same refers for Cd^{2+}). Furthermore, the physical adsorption of the metal ions onto soybean hulls' surface should also be taken into account. Similar observations were made in our previously published paper concerning the adsorption of Cd^{2+} onto lignocellulosic wood waste [2].

In the case of the adsorption of RY 39 and AB 225 dyes on the SH+PO and SH-PO, the optimal dye removal was obtained in an acidic medium (pH =3), (see Figure 6). At pH < 3, lower removal percentages could be observed, while at higher pH, a drastic decline is noticed (except for the removal AB 225 by SH-PO). Taking into account the microstate distribution charts for RY 39 and AB 225 (Supplementary material,

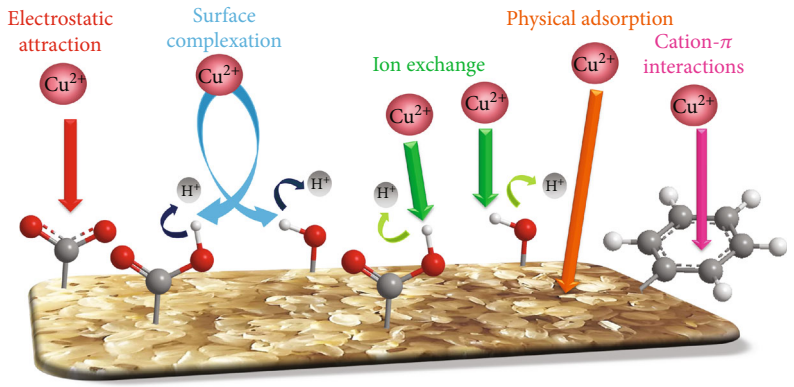

Figure 5: Graphical interpretation of the possible interaction between Cu^{2+} and soybean hulls' surface.

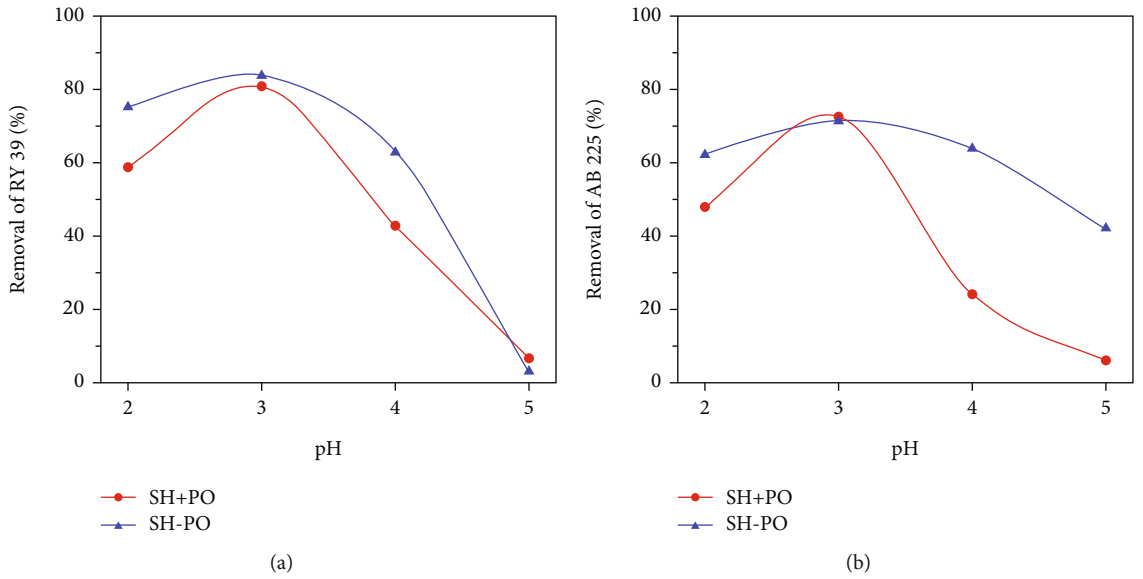

Figure 6: Effect of solution pH on (a) RY 39 and (b) AB 225 removal by soybean hulls.

see Figures S1c and S2c), it can be concluded that in the investigated pH range (2-5), dyes do not undergo structural changes (dominant microstates are present almost 100%), which further implicates that adsorption is principally governed by the pH-induced changes of the adsorbent surface. This is evidenced by the fact that the dye removal trends comply with the soybean hulls' zeta potential (see Figure 3(b)). Furthermore, considering dye removal (see Figure 6), it is clear that similar trends are obtained indicating that analogous adsorbent functionalities are responsible for the dye-adsorbent interactions for both dyes. As presented in Figure 3(b), it is obvious that SH+PO and SH-PO are positively charged at pH below 2.55 and 2.36, respectively, while above these values, the adsorbents' surfaces are negative. The increased adsorption of the dyes on going from pH = 2 to 3 could only suggest that stronger interactions of the dyes are established with a negatively charged adsorbent. According to the predicted dyes' pK_a values (Supplementary material, see Figure S1 and S2), it is clear that at pH 3, both dyes bear negative charges (*i.e.*, their sulfonic groups are deprotonated). Since the surfaces of SH+PO and SH-PO at this pH value are negative (see Figure 3(b)), it is justified to assume that the electrostatic repulsion between dyes and adsorbents dictates the orientation of the dye molecules (see Figure 7). This happens in such a way that a negative dye charge is raised away from the negative adsorbent surface enabling groups on the opposite side to interact with the adsorbent surface through multiple hydrogen interactions. A further increase of the solution's pH value causes the decline of the dye removal, probably due to the competition of the negatively charged dyes with solution OH^- groups, leading to a more disordered system preventing dyes to orientate in such a way to achieve effective interactions with an adsorbent. Also, the swelling of the soybean hulls causes the lowering of the zeta potential, *i.e.*, its negative value, affecting the degree of the effectively established interactions. In general, it could be suggested that dye adsorption is closely related to the extent of an adsorbent negative charge.

By comparing the adsorption capacities of SH+PO and SH-PO at pH = 3, it could be observed that no significant improvement is attained after the peroxidase extraction,

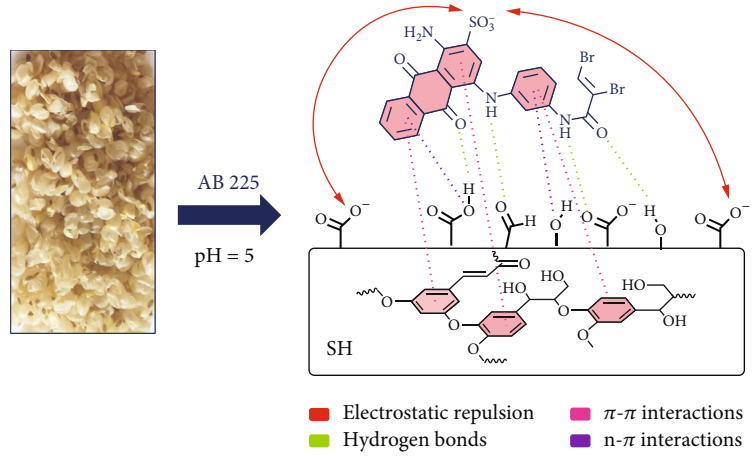

Figure 7: Graphical interpretation of the possible interaction of AB 225 and soybean hulls' surface.

while for other solution pH values, better adsorption is obtained for SH-PO, especially for AB 225 at pH > 3 (see Figure 6). The differences between the removal of these dyes at a pH > 4 could be ascribed to their ionization states (Supplementary Material, see Figures S1 and S2), wherein the RY 39 bears a double negative charge and, as such, the repulsion with the excess of OH^- is more pronounced with respect to AB 225 (having one anionic group), thus suppressing the effective adsorption of RY 39.

The detailed observations regarding the soybean hulls' ATR-FTIR spectra recorded before and after dye adsorption (Supplementary Material, see Figure S4) led us to conclude that dye adsorption is governed by the repulsion between its negative charges and the adsorbent surface and is attained by the cooperation of the different interactions such as hydrogen bonds, π-π stacking, and n-π interactions [15] (see Figure 7, displayed for AB 225, the same refers for RY 39). Multiple strong hydrogen bonds could be established between dye carbonyl groups with O–H groups (hydroxyl and carboxyl), as well as between dye N–H groups and adsorbent surface carbonyl groups (aldehyde, carbonyl, and carboxylate) (see Figure 7). As both dyes bear aromatic rings, it is justified to presume that π-π stacking interactions are formed with the aromatic monomer units (guaiacyl, syringyl, and *p*-hydroxyphenyl) of the lignin moieties [15, 42]. Considering the fact that adsorbent surface groups bear electron-rich oxygen atoms (such as O–H), the possible interaction mechanism may as well include n-π interactions with aromatic rings of the dyes [43].

For all further experiments, we have decided to use only soybean hulls without peroxidase (SH-PO) due to the following reasons:

(1) The observed higher metal ion removal by SH-PO than by SH+PO (see Figure 4).

(2) To "close the loop" and to reduce the disposal cost after peroxidase extraction. Namely, soybean peroxidase is widely used for the decolorization of textile industry wastewater [6, 44, 45] as well as for the degradation of phenolic compounds [46] in wastewater. However, in the available literature data, the authors did not discuss the soybean hulls' disposal after the peroxidase extraction, *i.e.* the soybean hulls remain as waste. In the current study, soybean hulls were recovered after the peroxidase extraction

(3) After the peroxidase extraction, the secondary pollution, *i.e.*, leaching of organic and inorganic matter in demineralized water from adsorbent is significantly lower in comparison with the adsorbent that did not undergo aqueous peroxidase extraction. More precisely, six times lower dichromate index (265.2 *vs.* 43.7 mg O_2/l) and five times lower total metal content (15.3 *vs.* 3.1 μg/l, Supplementary Material, see Table S1) were obtained in the sample which underwent peroxidase extraction than in the sample from which peroxidase was not extracted

3.3. Effect of Adsorbent Particle Size on the Removal of Metal Ions and Dyes. As given in the experimental part of this manuscript, the second step of adsorption optimization is to assess the effect of SH-PO particle size (710-1000 and 1000-1500 μm, *i.e.*, samples SH-PO1 and SH-PO2) on the removal of studied pollutants. From the results listed in Table 2, it is clear that Cd^{2+} and Cu^{2+} removal is slightly higher (for 4.2 and 11.0%, respectively) when the smaller adsorbent fraction was used (*i.e.*, SH-PO1). Such results are logical since for a given mass of adsorbent, the smaller adsorbent particle sizes have higher effective surface areas and therefore a higher number of available sites capable of binding metal ions [47, 48].

Interestingly, the soybean hulls' particle size did not have an impact on the percentage of removed dyes. Although the smaller fraction bears more active sites, no improvement in adsorption capacity is observed. Large dye molecules (Supplementary material, Figures S1a, and S2a) occupy a certain number of active sites, while at the same time they block unoccupied active sites due to their size, thus hindering the adsorption of other dye molecules. The obtained results are in line with the results presented by

Table 2: The influence of soybean hulls' particle sizes on the removal of pollutants.

Sample code	Removal of metal ions (%)		Removal of dyes (%)	
	Cd^{2+}	Cu^{2+}	RY 39	AB 225
SH-PO1	82.13	78.86	82.44	71.07
SH-PO2	78.68	70.00	81.98	71.90

Rizzuti and Lancaster [49], for the removal of Remazol Brilliant Blue R by the same adsorbent. Taking into account the results presented in Table 2, further kinetic, isotherm, thermodynamic and competitive experiments were conducted only for the sample SH-PO1.

3.4. Kinetic Studies. To gain detailed information about the pollutants' adsorption dynamic, their kinetics were studied, see Figure 8(a). At the beginning of the adsorption process, the pollutant removal sharply increased as time proceeded. This is due to a higher number of free sites having the ability for binding metal ions or dyes. The occurring phenomenon is more prominent in the case of dye removal than in the case of metal ion removal. Namely, after 30 min of contact time, about 92% and 88% of RY 39 and AB 225 were removed, while for the same time, about 80% and 69% of Cd^{2+} and Cu^{2+} were removed. By extending the contact time, the pollutant removal increased whereas the number of available sites decreased, reaching a plateau. Additionally, the effect of repulsive forces between pollutants in the solution and those adsorbed should not be neglected, since, by extending the contact time, they could hinder the pollutant's diffusion into the adsorbent structure [14]. Furthermore, the data presented in Figure 8(a) indicate that the adsorption process can be considered rapid since the equilibrium of dye removal was attained after 90 min of contact time, while in the case of metal ion removal, 120 min were sufficient for reaching equilibrium.

With the aim to obtain more information regarding the adsorption processes studied in this work, pseudo-first and pseudo-second-order kinetic models were tested. The linear fitting of $\log(q_t - q_e)$ *vs.* time and t/q_t *vs.* time plots (see Figures 8(b) and 8(c)) provided the kinetic parameters ($q_{e,\mathrm{cal}}$, k_1, and k_2), shown in Table 3. To select the best kinetic model that describes the adsorption processes, the corresponding coefficients of determination (R^2), together with the comparison between the experimental adsorption capacities at the equilibrium ($q_{e,\mathrm{exp}}$) and those obtained by applying the kinetic equations ($q_{e,\mathrm{cal}}$), were considered in parallel. Namely, from Figures 8(b) and 8(c) and Table 3, it is evident that the adsorption of metal ions and dyes follows a pseudo-second-order reaction, whereby the $q_{e,\mathrm{cal}}$ values for pseudo-second-order comply well with the experimentally obtained values. According to Ayele et al. [50], the primary rate-determining step is the adsorption rate of pseudo-second-order that relies on chemisorption or chemical adsorption.

The results presented in this section are comparable with those given in the literature. Namely, the pseudo-second-order is the most suitable for describing the Pb^{2+} adsorption onto 3-aminopropyltrietoxysilane-modified soybean and peanut hulls [51], Cd^{2+} and Pb^{2+} adsorption from a single and binary mixture onto soybean hulls [52], and azo dye safranin adsorption onto soybean hulls [53]. It has to be underlined that in the adsorption experiments carried out in the current study, special attention has been paid to secondary pollution during adsorption, *i.e.*, the peroxidase was first extracted and then the soybean hulls were used as an adsorbent, which is not the case in the previously mentioned papers.

Since the pseudo-first and pseudo-second-order kinetic models cannot identify the diffusion mechanism during the adsorption process, the kinetic data were further examined by the intraparticle diffusion model (see Table 4). Concerning the fact that several factors participate in pollutants' adsorption, the SH-PO1 intraparticle diffusion plots are not linear over the whole $t^{1/2}$ range, making it necessary to separate them into three linear zones, Figure 9.

The first linear zone observed at a low $t^{1/2}$ range is assigned to external surface adsorption in which the diffusion rate constant (k_1) is higher than in the other two zones (k_2 and k_3), *i.e.*, a quite fast adsorption occurred due to the well-shaken system. The second linear zone noticed at the intermediate $t^{1/2}$ range is attributed to the macropores' intraparticle diffusion. The last linear zone ($k_3 = 0.0001\text{-}0.0106\,\mathrm{mg/g\,min^{1/2}}$, see Table 4) is attributed to micropore diffusion, in which intraparticle diffusion starts to slow down as a result of low solute concentration in the solution. The greatest effect of the boundary layer on the adsorption was noticed in the third zone since C_3 is higher than C_1 and C_2 [47]. The observed increased resistance during the second and third phases (*i.e.*, $C_1 < C_2 < C_3$) can be explained by the fact that adsorbate diffusion and its kinetics are governed by Fick's law, *i.e.*, the transport rate is a function of the adsorbate gradient which is the highest during the first phase of the adsorption experiment and decreases as the experiment proceeds [54]. Negative values of the C_1 in the case of RY 39 and AB 225 indicate the effect of external film diffusion resistance in the adsorption initial stage [55]. Moreover, the lines do not pass through the origin, and therefore, the intraparticle diffusion is not the only rate-limiting step [56]; other processes may control the adsorption rate of Cd^{2+}, Cu^{2+}, RY 39, or AB225 onto SH-PO1.

3.5. Isotherm Studies. In order to better understand profoundly the interactions among the studied pollutants and the SH-PO1, the equilibrium adsorption experiments were performed at different initial pollutant concentrations. As given in Figure 10(a), SH-PO1 uptake capacity increases with increasing the initial pollutant concentration which could be ascribed to the high driving force for mass transfer at a high initial pollutant concentration. Bulut and Aydın

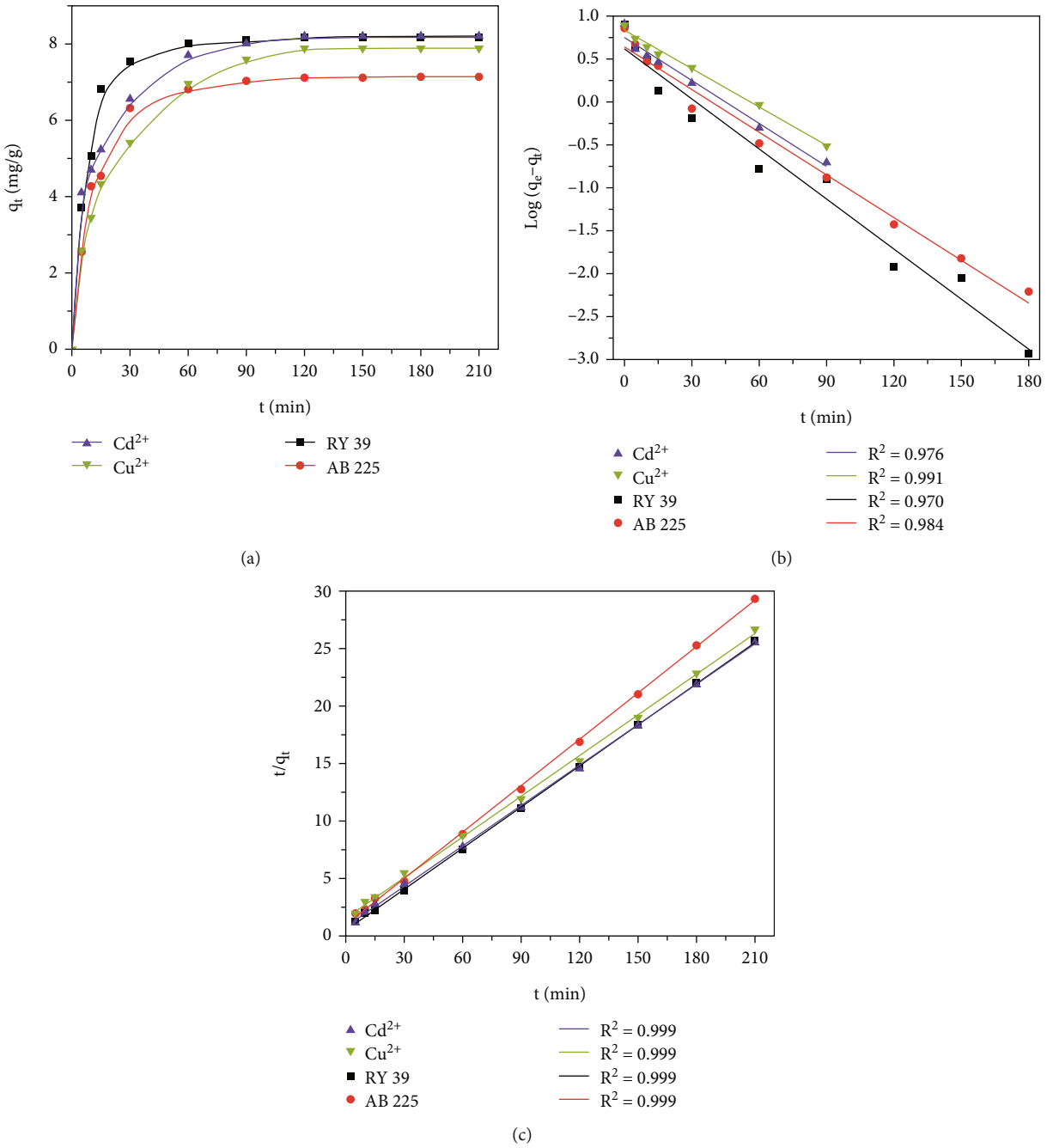

Figure 8: (a) Adsorption kinetic data and linear fit with (b) pseudo-first and (c) pseudo-second-order kinetic.

Table 3: Kinetic models' equations and kinetic parameters obtained by the pseudo-first- and pseudo-second-order kinetic models for metal ions and dye adsorption onto SH-PO1.

Kinetic models	Kinetic parameters	Cd^{2+}	Cu^{2+}	RY 39	AB 225
Pseudo-first kinetic model $\log(q_e - q_t) = \log q_e - (k_1/2.303)\bullet t$	$q_{e,cal}$	5.71	6.66	4.24	4.39
	k_1	0.038	0.034	0.044	0.038
Pseudo-second kinetic model $t/q_t = \left(1/\left(k_2 \bullet q_e^2\right)\right) + (1/q_e)\bullet t$	$q_{e,cal}$	8.57	8.51	8.40	7.46
	k_2	0.016	0.009	0.026	0.018
	$q_{e,\,exp}$	8.21	7.89	8.18	7.15

$q_e = q_{e,\,exp}$ and q_t (mg/g) are the amounts of pollutant adsorbed per gram adsorbent at equilibrium and at time t (min), $q_{e,cal}$ is the calculated amount of pollutant adsorbed per gram of adsorbent (mg/g), k_1 (1/min) is the pseudo-first-order rate constant, and k_2 (g/mg min) is the pseudo-second-order rate constant.

Table 4: Intraparticle diffusion model's equation and kinetic parameters for metal ions and dye adsorption onto SH-PO1.

Sample code	Intraparticle diffusion model $q_t = k_i \bullet t^{1/2} + C$								
	Zone I			Zone II			Zone III		
	k_1	C_1	R_1^2	k_2	C_2	R_2^2	k_3	C_3	R_3^2
Cd^{2+}	0.7616	2.34	0.994	0.1573	6.50	0.990	0.0009	8.21	0.999
Cu^{2+}	0.8786	0.70	0.978	0.2931	4.72	0.955	0.0009	7.88	0.999
RY 39	1.8682	-0.57	0.953	0.1182	7.00	0.795	0.0001	8.18	0.988
AB 225	1.2534	-0.09	0.792	0.1760	5.38	0.950	0.0106	7.00	0.896

q_t (mg/g) is the amount of pollutant adsorbed per gram adsorbent at time t (min), k_i (mg/g $min^{1/2}$) is the interparticle diffusion rate constant, and C is the parameter proportional to the extent of the boundary layer thickness (mg/g).

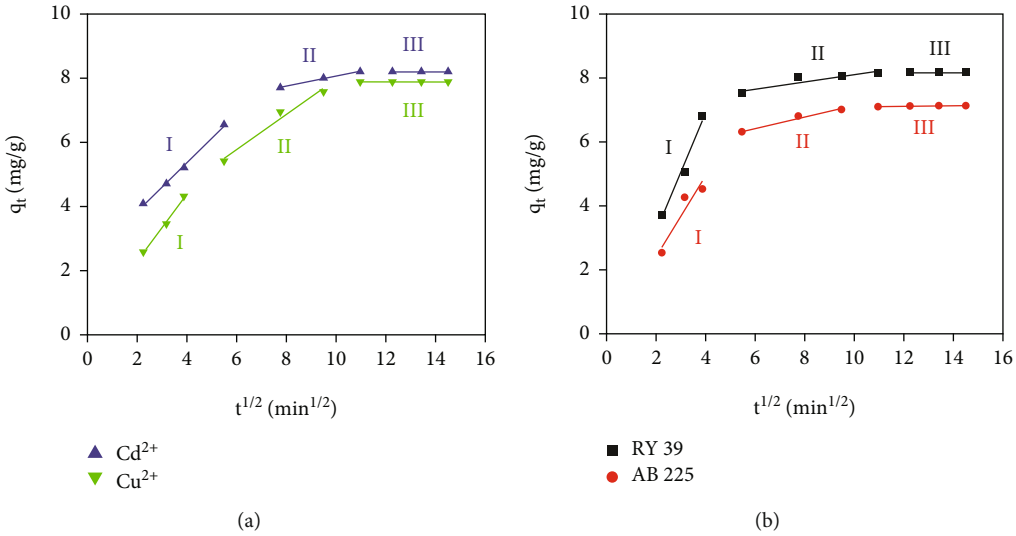

Figure 9: Intraparticle diffusion plots of the metal ions and dyes onto SH-PO1.

[57] and Ivanovska et al. [2, 58] observed the same behavior during isotherm experiments for methylene blue adsorption onto wheat shells; cadmium ion adsorption onto wood waste, nickel, and copper; and zinc ion adsorption onto jute fabrics, respectively. It has to be noted that at the initial pollutant concentrations above 25 mg/l, the SH-PO1 possessed around 25% higher uptake capacity for metal ions than for the dyes (see Figure 10(a)).

The obtained equilibrium data were further analyzed by using linearized forms of the Langmuir and Freundlich isotherm models (see Figures 10(b) and 10(c) and Table 5). The data fitting based on Langmuir isotherm showed higher R^2 values for all the pollutants. Thus, it can be stated that this model provided a better description of the studied system than the Freundlich model. Better fitting with the Langmuir model implies a monolayer pollutant adsorption onto an adsorbent surface having a finite number of uniformly distributed adsorption sites and homogeneous adsorption [53], which is in accordance with the results presented by Yu et al. [59].

The theoretical maximal adsorption capacities (q_m) of SH-PO1 determined by Langmuir modeling are 21.10, 20.54, 16.54, and 17.23 mg/g for Cd^{2+}, Cu^{2+}, RY 39, and AB 225, respectively (see Table 5). Depending on the Langmuir constant (K_L) value, the adsorption process could be evaluated as irreversible ($K_L = 0$), favorable ($0 < K_L < 1$), linear ($K_L = 1$), or unfavorable ($K_L > 1$). The values of K_L for all studied pollutants ranged between 0 and 1, pointing out the favorable adsorption. Slightly higher values of K_L observed for metal ions than for dyes suggested a slightly stronger interaction between SH-PO1 and metal ions than between SH-PO1 and dyes.

3.6. Thermodynamic Studies. Thermodynamic experiments were carried out at three different temperatures, 25, 35, and 45°C, *i.e.*, 298.15, 308.15, and 318.15 K, while the other optimized adsorption parameters are listed in Table 1. The results presented in Figure 11 revealed that by increasing the temperature from 25 to 45°C, the adsorption of all studied pollutants increases which could be explained by the increased availability of SH-PO1 surface sites and the pollutant mobility at higher temperatures [60]. This behavior is the most prominent for AB 225; its adsorption capacity increased by about 20%.

From the temperature-dependent study of Cd^{2+}, Cu^{2+}, RY 39, and AB 225 adsorption onto SH-PO1, the thermodynamic parameters standard enthalpy ΔH^0, standard entropy ΔS^0, and standard Gibbs energy change ΔG^0 were calculated (see Table 6). At the system equilibrium, the obtained positive values of ΔS^0 imply an increase of randomness at the

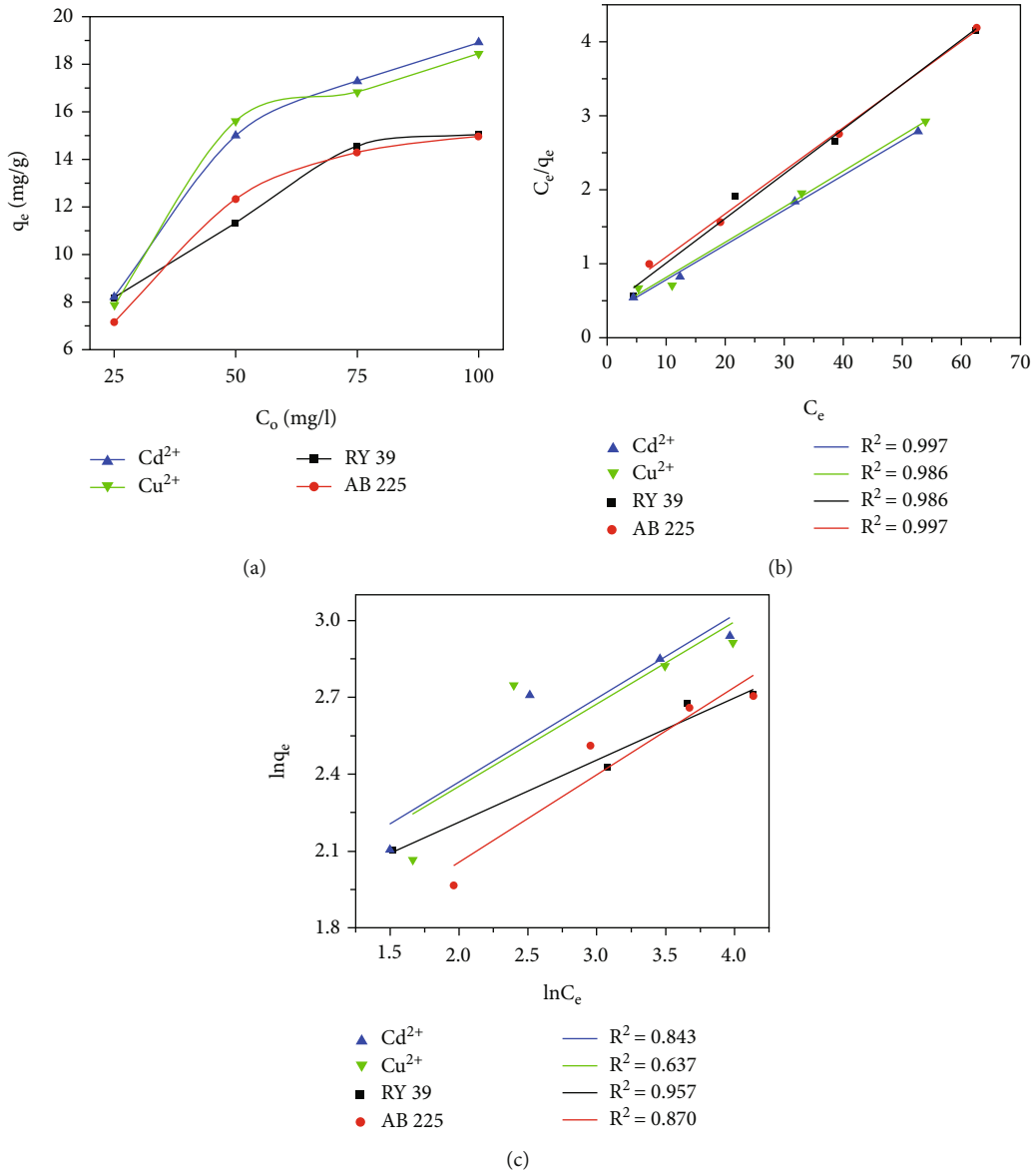

Figure 10: (a) Equilibrium pollutant adsorption onto SH-PO1 and (b) Langmuir and (c) Freundlich adsorption isotherms and the linear fit of experimental adsorption data for different pollutants.

Table 5: Isotherm models' equations and obtained isotherm parameters for metal ions and dyes adsorption onto SH-PO1.

Adsorption isotherms	Isotherm parameters	Sample code			
		Cd^{2+}	Cu^{2+}	RY 39	AB 225
Langmuir $C_e/q_e = (1/(q_m \bullet K_L)) + (1/q_m) \bullet C_e$	K_L	0.159	0.158	0.152	0.113
	q_m	21.10	20.54	16.54	17.23
Freundlich $\ln q_e = \ln K_f + (1/n) \bullet \ln C_e$	K_f	5.56	5.54	5.61	3.94
	$1/n$	0.327	0.321	0.243	0.342

$q_e = q_{e,\,\mathrm{exp}}$ (mg/g) is equilibrium pollutant concentration per gram of adsorbent, q_m (mg/g) is a maximal adsorbed pollutant per gram of adsorbent, K_L (l/mg) is Langmuir constant, C_e (mg/l) is the equilibrium pollutant concentration in the solution, K_f is the Freundlich constant (mg/g)/(l/mg)$^{1/n}$, and$1/n$ is the constant related to the fabric surface heterogeneity.

solid-solution interface, indicating that the adsorption of all considered pollutants is an entropy-driven process [61]. The positive ΔS^0 in a combination with the negative ΔG^0 suggest that their adsorption onto SH-PO1 is feasible and spontaneous [16]. Furthermore, the process is of endothermic character since the parameter ΔH^0 is positive.

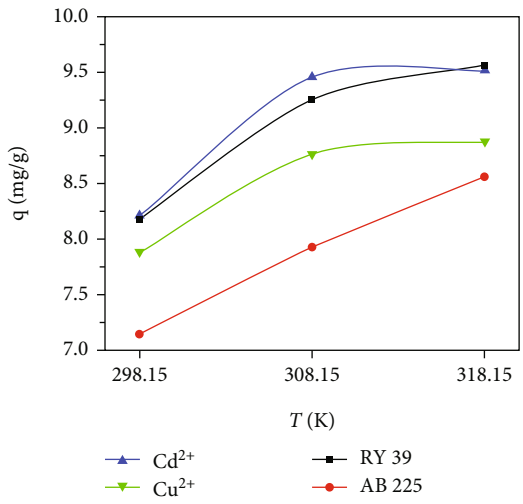

Figure 11: The effect of temperature on the pollutants' adsorption onto SH-PO1.

3.7. Competitive Adsorption of Metal Ions and Dyes. In real conditions, most of the wastewater contains a mixture of different pollutants such as metal ions and dyes, and therefore, the assessment of adsorbent overall performance is of great importance. To examine the simultaneous competitive adsorption of metals and dyes and the two tested metals and dyes onto SH-PO1, ten binary mixtures were prepared (see Table 7).

The Cd^{2+} removal from the binary mixtures containing RY 39 or AB 225 at a pH of 5.00 is almost the same as in the case of single pollutant adsorption (see Figure 4(a)). This is also observed for Cu^{2+} (see Figure 4(b)), where somewhat higher metal removal was observed during the competitive adsorption experiments. However, in the metal binary mixture, Cu^{2+} is more competitive than Cd^{2+} (removal of 71.01 *vs.* 20.96%). This is expected due to Cu^{2+} significantly lower molecular mass as well as higher effective ionic radii and electronegativity [62].

When the dye's removal from the single aqueous solution (see Figure 6) and binary mixtures (see Table 7) were compared, it is clear that the RY 39 and AB 225 removal from binary mixtures (at pH of 3.00) is not affected by the metal cosolute. The dye binary mixture results in lower adsorption of RY 39 with respect to the adsorption of single-dye solutions. This could be ascribed to the fact that the molecules of RY 39 are more rigid and bear double negative charge than the AB 225 molecule, which is smaller and thus can more easily diffuse through the solution. Surprisingly, the removal of RY 39 is significantly reinforced (more than 8 times) at pH = 5 in the presence of metal cosolute. One explanation could be that positive metal ions compensate for SH-PO1's surface negative charge and prevent repulsion between the negative dye and the soybean hull surface in that way. On the grounds of the previous statement, it is probable for RY 39 to establish stronger interactions being reflected through better adsorption onto SH-PO1. On the contrary, the presence of a co-solute (Cd^{2+}, Cu^{2+}, or RY 39) contributed to a higher AB 225 removal due to the previously described compensating metal ions' effect.

To summarize, SH-PO1 is the most efficient adsorbent for the mixture of AB 225 and Cu^{2+}, independent of the solution pH. Additionally, the lowest adsorbent affinity was registered for the mixture containing both metal ions. These very interesting results promote the novel valorization of soybean hulls after peroxidase extraction as adsorbents for inorganic and organic pollutants and bring them into the circular economy.

3.8. Advantages and Future Perspective of Soybean Hulls. It seems this is the right place to discuss the advantages of the studied SH-PO over the well-known conventional adsorbents such as activated carbons, ion exchange resins, and zeolites. SH-PO and other nonconventional adsorbents are competitive with the mentioned conventional adsorbents since they are low cost and abundant and have high affinity, capacity, rate of adsorption, and selectivity for different pollutant concentrations [63, 64]. Having a wide variety of functional groups, nonconventional adsorbents such as SH-PO provide intrinsic chelating and complexing properties for different pollutants including heavy metals, dyes, and aromatic compounds and can reduce their concentrations to ppb levels. The regeneration of nonconventional adsorbents in washing solvents is very easy since; as it was mentioned, the interaction between the pollutant and adsorbent is driven mainly by electrostatic attraction, stacking interactions, and ion exchange. On the other hand, the utilization of activated carbons as adsorbents is restricted due to the high cost of the precursor (such as petroleum residues and some commercial polymers) and the rapid saturation that imposes the necessity for their regeneration (which is expensive, complicated, results in loss of the adsorbent, and is energy-consuming) and incineration [65]. The activated carbons are nonselective and ineffective for disperse and vat dyes requiring the utilization of complexing agents to improve their removal performance [66]. Furthermore, most commercial ion exchange resins are derived from petroleum-based raw materials using processing chemistry that is not always safe and environmentally friendly. One of the highest drawbacks of this adsorbent is poor contact with the aqueous solution which requires its further modification and/or pretreatment by activation solvents. Generally speaking, activated carbons and synthetic resins suffer from a lack of selectivity, and their applications are often limited to low contaminant concentrations. Zeolites represent another group of conventional adsorbents that are used for various pollutants; however, they are characterized by low selectivity, while their microporous structure makes them unsuitable for bulky molecules [67].

The investigation of adsorbent stability, reusability, or regeneration was not within the focus of the current study, since the mentioned procedures decrease the adsorbent capacity and generate new wastewater, making them inappropriate for industrial wastewater [68]. Besides the SH-PO1 large adsorption capacities for different pollutants, the adsorption process produces solid waste that can cause secondary pollution. In light of that, the lifecycle of SH-PO1 with adsorbed pollutants could be extended by their further utilization for the production of bio-based composites which will be used as building materials

Table 6: Thermodynamic parameters for adsorption of different pollutants onto SH-PO1.

Pollutant	Temperature (K)	Thermodynamic parameters		
		ΔG^0 (kJ/mol)	ΔH^0 (kJ/mol)	ΔS^0 (J/mol K)
Cd^{2+}	298.15	-18.624	42.758	208.424
	308.15	-22.667		
	318.15	-23.713		
Cu^{2+}	298.15	-18.106	21.616	134.521
	308.15	-20.360		
	318.15	-21.315		
RY 39	298.15	-18.571	43.530	210.278
	308.15	-21.778		
	318.15	-24.005		
AB 225	298.15	-17.120	23.576	137.45
	308.15	-18.779		
	318.15	-20.555		

Table 7: Competitive adsorption from binary mixtures onto SH-PO1.

Pollutants	pH	Removal of metal ions (%)		Removal of dyes (%)	
		Cd^{2+}	Cu^{2+}	RY 39	AB 225
RY 39+Cd^{2+}	5.00	79.25	/	34.71	/
RY 39+Cu^{2+}		/	81.83	52.08	/
RY 39+Cd^{2+}	3.00	46.26	/	81.45	/
RY 39+Cu^{2+}		/	59.88	82.73	/
AB 225+Cd^{2+}	5.00	79.94	/	/	44.29
AB 225+Cu^{2+}		/	84.89	/	68.27
AB 225+Cd^{2+}	3.00	46.29	/	/	88.32
AB 225+Cu^{2+}		/	60.82	/	87.86
Cd^{2+}+Cu^{2+}	5.00	20.96	71.01		
RY 39+AB 225	3.00			60.98	70.27

or carbonized and used as a great alternative to porous carbon and a cathode matrix for lithium-sulfur batteries [69].

4. Conclusions

The experiments conducted in this study confirmed that the soybean hulls could be successfully recovered after peroxidase extraction and used as adsorbents for metal ions and dyes. The soybean hulls' adsorption potential for Cd^{2+}, Cu^{2+}, RY 39, and AB 225 from a single-pollutant solution changes depending on the pH, peroxidase extraction, adsorbent particle size, contact time, pollutant initial concentration, and temperature. Before peroxidase extraction, soybean hulls are capable of removing 72% Cd^{2+}, 71% Cu^{2+} (at a pH of 5.00) and 81% RY 39, 73% AB 225 (at a pH of 3.00), respectively. After peroxidase extraction, the removal of Cd^{2+} and Cu^{2+} increased by 14.6 and 10.9%, respectively. Soybean hulls without peroxidase possessed significantly lower secondary pollution (*i.e.*, six times lower dichromate index (265.2 *vs.* 43.7 mg O_2/l), and five times lower total metal content (15.3 *vs.* 3.1 μg/l) than those with peroxidase.

The adsorbent particle size did not affect the dye removal; however, Cd^{2+} and Cu^{2+} removal slightly increased when the smaller adsorbent fraction (710-1000 μm) was used. The adsorption of metal ions and dyes can be considered rapid since the equilibrium was attained after 120 min and 90 min of contact time, respectively. Furthermore, after 30 min of contact time, 92% and 88% of RY 39 and AB 225 were removed, while after the same time, 80% and 69% of Cd^{2+} and Cu^{2+} were removed. The adsorption of all tested pollutants follows a pseudo-second-order reaction (through the fast adsorption, intraparticle diffusion, and final equilibrium stage) indicating that chemical adsorption is the velocity limiting factor. On the other hand, better fitting with the Langmuir model implies a uniform distribution of adsorption sites and the presence of a single layer of pollutant on the soybean hulls' surfaces. The maximal adsorption capacities determined by the Langmuir model are 21.10, 20.54, 16.54, and 17.23 mg/g for Cd^{2+}, Cu^{2+}, RY 39, and AB 225, respectively. Calculated thermodynamic parameters suggested that the adsorption of all pollutants is spontaneous and of endothermic character.

Taking into account that real wastewater contains a mixture of different pollutants, the simultaneous competitive adsorption of metals and dyes from binary mixtures was studied. The obtained results revealed that soybean hulls are the most efficient adsorbent for the mixture of AB 225 and Cu^{2+}. The findings of this study contributed to a novel valorization of soybean hulls and bring them into the circular economy concept.

Data Availability

Aleksandra Ivanovska (e-mail: aivanovska@tmf.bg.ac.rs) should be contacted to request the data.

Conflicts of Interest

The authors declare that there is no conflict of interest regarding the publication of this article.

Acknowledgments

The authors thank Nemanja Barać (Innovation Center of the Faculty of Technology and Metallurgy, University of Belgrade) for FE-SEM images, Matea Korica (Innovation Center of the Faculty of Technology and Metallurgy, University of Belgrade) for determination of fabric zeta potential, and Ilija Cvijetić (Faculty of Chemistry, University of Belgrade) for the determination of dye pK_a values. This work was supported by the Ministry of Education, Science and Technological Development of the Republic of Serbia (Contract No. 451-03-47/2023-01/200287, 451-03-47/2023-01/200135, 451-03-47/2023-01/200161, and 451-03-68/2022-14/200026).

Supplementary Materials

This manuscript contains supplementary material: Figure S1: (a) RY 39 dye structure with its pK_a values (marked in red), (b) major protonation states, and (c) distribution chart. Figure S2: (a) AB 225 dye structure with its pK_a values (marked in red), (b) major protonation states, and (c) distribution chart. Table S1: comparison between the metal concentration in demineralized water and in the water after immersing the soybean hulls at a pH of 3.00 for 24 h. Figure S3: ATR-FTIR spectra of SH-PO before and after the adsorption of Cd^{2+} or Cu^{2+}. Figure S4: ATR-FTIR spectra of SH-PO before and after the adsorption of RY 39 or AB 225. *(Supplementary Materials)*

References

[1] A. K. Flores-Trujillo, P. Mussali-Galante, M. C. de Hoces et al., "Biosorption of heavy metals on *Opuntia fuliginosa* and *Agave angustifolia* fibers for their elimination from water," *International journal of Environmental Science and Technology*, vol. 18, no. 2, pp. 441–454, 2021.

[2] A. Ivanovska, S. Veljović, B. Dojčinović et al., "A strategy to revalue a wood waste for simultaneous cadmium removal and wastewater disinfection," *Adsorption Science and Technology*, vol. 2021, article 3552300, pp. 1–14, 2021.

[3] D. Đukić-Ćosić, K. Baralić, D. Javorac et al., "Exploring the relationship between blood toxic metal(oid)s and serum insulin levels through benchmark modelling of human data: possible role of arsenic as a metabolic disruptor," *Environmental Research*, vol. 215, article 114283, 2022.

[4] K. Baralić, D. Javorac, Đ. Marić et al., "Benchmark dose approach in investigating the relationship between blood metal levels and reproductive hormones: data set from human study107313," *Environment International*, vol. 165, 2022.

[5] A. Buha, K. Baralić, D. Djukic-Cosic et al., "The role of toxic metals and metalloids in Nrf2 signaling," *Antioxidants*, vol. 10, p. 630, 2021.

[6] M. Svetozarević, N. Šekuljica, Z. Knežević-Jugović, and D. Mijin, "Agricultural waste as a source of peroxidase for wastewater treatment: insight in kinetics and process parameters optimization for anthraquinone dye removal," *Environmental Technology and Innovation*, vol. 21, article 101289, 2021.

[7] A. G. Varghese, S. A. Paul, and M. S. Latha, "Remediation of heavy metals and dyes from wastewater using cellulose-based adsorbents," *Environmental Chemistry Letters*, vol. 17, no. 2, pp. 867–877, 2019.

[8] A. Ahmad and T. Azam, "4- water purification technologies," in *Bottled and Packaged Water*, A. M. Grumezescu and A. M. Holban, Eds., pp. 83–120, Woodhead Publishing, 2019.

[9] M. Bhowmik, A. Debnath, and B. Saha, "Scale-up design and treatment cost analysis for abatement of hexavalent chromium and Metanil Yellow dye from aqueous solution using mixed phase $CaFe_2O_4$ and ZrO_2 nanocomposite," *International Journal of Environmental Research*, vol. 16, p. 80, 2022.

[10] P. Das, S. Nisa, A. Debnath, and S. Biswajit, "Enhanced adsorptive removal of toxic anionic dye by novel magnetic polymeric nanocomposite: optimization of process parameters," *Journal of Dispersion Science and Technology*, vol. 43, no. 6, pp. 880–895, 2022.

[11] N. M. Mahmoodi, M. Oveisi, M. Bakhtiari et al., "Environmentally friendly ultrasound-assisted synthesis of magnetic zeolitic imidazolate framework - graphene oxide nanocomposites and pollutant removal from water," *Journal of Molecular Liquids*, vol. 282, pp. 115–130, 2019.

[12] F. Hosseini, S. Sadighian, H. Hosseini-Monfared, and N. M. Mahmoodi, "Dye removal and kinetics of adsorption by magnetic chitosan nanoparticles," *Desalination and Water Treatment*, vol. 57, no. 51, pp. 24378–24386, 2016.

[13] N. Blagojev, D. Kukić, V. Vasić, M. Šćiban, J. Prodanović, and O. Bera, "A new approach for modelling and optimization of Cu(II) biosorption from aqueous solutions using sugar beet shreds in a fixed-bed column," *Journal of Hazardous Materials*, vol. 363, pp. 366–375, 2019.

[14] A. Ivanovska, L. Pavun, B. Dojčinović, and M. Kostić, "Kinetic and isotherm studies for nickel ions' biosorption by jute fabrics," *Journal of the Serbian Chemical Society*, vol. 86, no. 9, pp. 885–897, 2021.

[15] A. Ivanovska, J. Lađarević, L. Pavun et al., "Obtaining jute fabrics with enhanced sorption properties and "closing the loop" of their lifecycle," *Industrial Crops and Products*, vol. 171, p. 113913, 2021.

[16] A. Ivanovska, I. Branković, J. Lađarević, L. Pavun, and M. Kostic, "Oxidized jute as a valuable adsorbent for Congo Red from an aqueous solution," *Journal of Engineered Fibers and Fabrics*, vol. 17, pp. 1–9, 2022.

[17] C. Mongioví, N. Morin-Crini, D. Lacalamita et al., "Biosorbents from plant fibers of hemp and flax for metal removal: comparison of their biosorption properties," *Molecules*, vol. 26, p. 4199, 2021.

[18] N. Mladenovic, P. Makreski, A. Tarbuk et al., "Improved dye removal ability of modified rice husk with effluent from alkaline scouring based on the circular economy concept," *Processes*, vol. 8, p. 653, 2020.

[19] R. A. Khera, M. Iqbal, S. Jabeen et al., "Adsorption efficiency of Pitpapra biomass under single and binary metal systems," *Surfaces and Interfaces*, vol. 14, pp. 138–145, 2019.

[20] D. Schwantes, A. C. Goncalves, A. De Varennes, and A. L. Braccini, "Modified grape stem as a renewable adsorbent for cadmium removal," *Water Science and Technology*, vol. 78, no. 11, pp. 2308–2320, 2018.

[21] A. Ivanovska, S. Veljović, M. Reljić et al., "Closing the loop: dyeing and adsorption potential of mulberry wood waste," *Journal of Natural Fibers*, vol. 19, no. 15, pp. 11050–11063, 2021.

[22] A. Stavrinou, C. A. Aggelopoulos, and C. D. Tsakiroglou, "Exploring the adsorption mechanisms of cationic and anionic dyes onto agricultural waste peels of banana, cucumber and potato: adsorption kinetics and equilibrium isotherms as a tool," *Journal of Environmental Chemical Engineering*, vol. 2, no. 6, pp. 6958–6970, 2018.

[23] M. U. Farooq, M. I. Jalees, A. Iqbal, N. Zahra, and A. Kiran, "Characterization and adsorption study of biosorbents for the removal of basic cationic dye: kinetic and isotherm analysis," *Desalination and Water Treatment*, vol. 160, pp. 333–342, 2019.

[24] World Health Organization, "Action is needed on chemicals of major public health concern," 2010, November 2022, https://www.who.int/news-room/photo-story/photo-story-detail/10-chemicals-of-public-health-concern.

[25] A. Buha, D. Wallace, V. Matovic et al., "Cadmium exposure as a putative risk factor for the development of pancreatic cancer: three different lines of evidence," *BioMed Research International*, vol. 2017, Article ID 1981837, 8 pages, 2017.

[26] V. R. Djordjevic, D. R. Wallace, A. Schweitzer et al., "Environmental cadmium exposure and pancreatic cancer: evidence from case control, animal and in vitro studies," *Environmental International*, vol. 128, pp. 353–361, 2019.

[27] A. Pizent, M. Anđelković, B. T. Lovaković et al., "Environmental exposure to metals, parameters of oxidative stress in blood and prostate cancer: results from two cohorts," *Antioxidants*, vol. 11, no. 10, p. 2044, 2022.

[28] A. Mudhoo, V. K. Garg, and S. Wang, "Removal of heavy metals by biosorption," *Environmental Chemistry Letters*, vol. 10, no. 2, pp. 109–117, 2011.

[29] Y. Han, J. Li, B. He, and L. Li, "Preparation and characterization of a novel ACF-TpPa-1 composite for dye adsorption," *Journal of Engineered Fiber and Fabrics*, vol. 16, pp. 1–10, 2021.

[30] M. M. Svetozarević, N. Šekuljica, Z. Knežević-Jugović, and D. Mijin, "Optimization and kinetic study of anthraquinone dye removal from colored wastewater using soybean seed as a source of peroxidase for environmental welfare," *Macedonian Journal of Chemistry and Chemical Engineering*, vol. 39, no. 2, pp. 197–206, 2020.

[31] T. Auxenfans, D. Crônier, B. Chabbert, and G. Paës, "Understanding the structural and chemical changes of plant biomass following steam explosion pretreatment," *Biotechnology for Biofuels*, vol. 10, p. 36, 2017.

[32] A. Ivanovska and M. Kostić, "Electrokinetic properties of chemically modified jute fabrics," *Journal of the Serbian Chemical Society*, vol. 85, no. 12, pp. 1621–1627, 2020.

[33] APHA, AWWA, and WPCF, *Standard Methods for the Examination of Water and Wastewater, Method 5220 C*, Chemical oxygen demand (COD), Washington, DC, 20th edition, 1998.

[34] M. L. Tummino, V. Tolardo, M. Malandrino, R. Sadraei, G. Magnacca, and E. Laurenti, "A way to close the loop: physicochemical and adsorbing properties of soybean hulls recovered after soybean peroxidase extraction," *Frontiers in Chemistry*, vol. 8, p. 763, 2020.

[35] L. F. Cusioli, H. B. Quesada, A. T. A. Baptista, R. G. Gomes, and R. Bergamasco, "Soybean hulls as a low-cost biosorbent for removal of methylene blue contaminant," *Environmental Progress and Sustainable Energy*, vol. 39, no. 2, article e13328, 2020.

[36] J. Široký, R. S. Blackburn, T. Bechtold, J. Taylor, and P. White, "Attenuated total reflectance Fourier-transform infrared spectroscopy analysis of crystallinity changes in lyocell following continuous treatment with sodium hydroxide," *Cellulose*, vol. 17, no. 1, pp. 103–115, 2009.

[37] A. M. Rizzuti, F. L. Ellis, and L. W. Cosme, "Biosorption of mercury from dilute aqueous solutions using soybean hulls and rice hulls," *Waste and Biomass Valorization*, vol. 6, no. 4, pp. 561–568, 2015.

[38] J. D. Cuppett, S. E. Duncan, and A. M. Dietrich, "Evaluation of copper speciation and water quality factors that affect aqueous copper tasting response," *Chemical Senses*, vol. 31, no. 7, pp. 689–697, 2006.

[39] S. E. Sanni, J. O. Odigure, M. E. Emetere, E. E. Okoro, O. Agboola, and Y. O. Sherif, "Decontamination of wastewater effluent using sugar cane bagasse and soybean hulls," *Journal of Physics: Conference Series*, vol. 1378, p. 022047, 2019.

[40] X. Yang, Y. Wan, Y. Zheng et al., "Surface functional groups of carbon-based adsorbents and their roles in the removal of heavy metals from aqueous solutions: a critical review," *Chemical Engineering Journal*, vol. 366, pp. 608–621, 2019.

[41] P. Yang, L. Yang, Y. Wang, L. Song, J. Yang, and G. Chang, "An indole-based aerogel for enhanced removal of heavy metals from water *via* the synergistic effects of complexation and cation-π interactions," *Journal of Materials Chemistry A*, vol. 7, no. 2, pp. 531–539, 2019.

[42] P. C. Bhomick, A. Supong, M. Baruah, C. Pongener, C. Gogoi, and D. Sinha, "Alizarin Red S adsorption onto biomass-based activated carbon: optimization of adsorption process parameters using Taguchi experimental design," *International journal of Environmental Science and Technology*, vol. 17, no. 2, pp. 1137–1148, 2020.

[43] F. Mashkoor and A. Nasar, "Magnetized Tectona grandis sawdust as a novel adsorbent: preparation, characterization, and utilization for the removal of methylene blue from aqueous solution," *Cellulose*, vol. 27, no. 5, pp. 2613–2635, 2020.

[44] L. G. Cordova-Villegas, A. Y. Cordova-Villegas, K. E. Taylor, and N. Biswas, "Response surface methodology for optimization of enzyme-catalyzed azo dye decolorization," *Journal of Environmental Engineering*, vol. 145, no. 5, article 04019013, 2019.

[45] M. Svetozarević, N. Šekuljica, A. Onjia et al., "Biodegradation of synthetic dyes by free and cross-linked peroxidase in microfluidic reactor," *Environmental Technology and Innovation*, vol. 26, p. 102373, 2022.

[46] V. Tolardo, S. García-Ballesteros, L. Santos-Juanes et al., "Pentachlorophenol removal from water by soybean peroxidase and iron(II) salts concerted action," *Water, Air, & Soil Pollution*, vol. 230, no. 6, p. 140, 2019.

[47] E.-K. Guechi and O. Hamdaoui, "Evaluation of potato peel as a novel adsorbent for the removal of cu(II) from aqueous solutions: equilibrium, kinetic, and thermodynamic studies," *Desalination and Water Treatment*, vol. 57, no. 23, pp. 10677–10688, 2015.

[48] G. M. Al-Senani and F. F. Al-Fawzan, "Study on adsorption of Cu and Ba from aqueous solutions using nanoparticles of *Origanum* (OR) and *Lavandula* (LV)," *Bioinorganic Chemistry and Applications*, vol. 2018, Article ID 3936178, 8 pages, 2018.

[49] A. M. Rizzuti and D. J. Lancaster, "Utilizing soybean hulls and rice hulls to remove textile dyes from contaminated water," *Waste and Biomass Valorization*, vol. 4, no. 3, pp. 647–653, 2013.

[50] A. L. Ayele, B. Z. Tizazu, and A. B. Wassie, "Chemical modification of *Teff* straw biomass for adsorptive removal of Cr (VI) from aqueous solution: characterization, optimization, kinetics, and thermodynamic aspects," *Adsorption Science and Technology*, vol. 2022, article 5820207, pp. 1–25, 2022.

[51] Z. Ding, E. Yu, Z. Hu, and Y. Zhang, "Removal of aqueous Pb (II) using low-cost agricultural waste modified by 3-aminopropyltrimethoxysilane," *Asian Journal of Chemistry*, vol. 27, no. 5, pp. 1805–1810, 2015.

[52] A. N. Módenes, F. R. Espinoza-Quiñones, A. Colombo, C. L. Geraldi, and D. E. G. Trigueros, "Inhibitory effect on the uptake and diffusion of Cd2+ onto soybean hull sorbent in cd-Pb binary sorption systems," *Journal of Environmental Management*, vol. 154, pp. 22–32, 2015.

[53] V. Chandane and V. K. Singh, "Adsorption of safranin dye from aqueous solutions using a low-cost agro-waste material soybean hull," *Desalination and Water Treatment*, vol. 57, no. 9, pp. 4122–4134, 2014.

[54] A. Sharaf and Y. Liu, "Mechanisms and kinetics of greywater treatment using biologically active granular activated carbon," *Chemosphere*, vol. 263, p. 128113, 2021.

[55] Q. Zhu, G. D. Moggridge, and C. D'Agostino, "Adsorption of pyridine from aqueous solutions by polymeric adsorbents MN 200 and MN 500. Part 2: kinetics and diffusion analysis," *Chemical Engineering Journal*, vol. 306, pp. 1223–1233, 2016.

[56] M. Rafatullah, O. Sulaiman, R. Hashim, and A. Ahmad, "Removal of cadmium (II) from aqueous solutions by adsorption using Meranti wood," *Wood Science and Technology*, vol. 46, no. 1-3, pp. 221–241, 2012.

[57] Y. Bulut and H. Aydın, "A kinetics and thermodynamics study of methylene blue adsorption on wheat shells," *Desalination*, vol. 194, no. 1-3, pp. 259–267, 2006.

[58] A. Ivanovska, B. Dojcinovic, S. Maletic, L. Pavun, K. Asanovic, and M. Kostic, "Waste jute fabric as a biosorbent for heavy metal ions from aqueous solution," *Fibers and Polymers*, vol. 21, no. 9, pp. 1992–2002, 2020.

[59] K. Ali, M. U. Javaid, Z. Ali, and M. J. Zaghum, "Biomass-derived adsorbents for dye and heavy metal removal from wastewater," *Adsorption Science and Technology*, vol. 2021, article 9357509, pp. 1–14, 2021.

[60] R. Yu, X. Hu, Z. Ding, and Y. Zhang, "Biosorption of lead(II) from aqueous solutions using adsorbents prepared from peanut hulls, soybean shells and grapefruit peels," *Environmental Engineering and Management Journal*, vol. 15, no. 11, pp. 2403–2411, 2016.

[61] D. Milošević, S. Lević, S. Lazarević et al., "Hybrid material based on subgleba of mosaic puffball mushroom (*Handkea utriformis*) as an adsorbent for heavy metal removal from aqueous solutions," *Journal of Environmental Management*, vol. 297, p. 113358, 2021.

[62] S. Loiacono, G. Crini, B. Martel et al., "Simultaneous removal of Cd, Co, Cu, Mn, Ni, and Zn from synthetic solutions on a hemp-based felt. II. Chemical modification," *Journal of Applied Polymer Science*, vol. 134, no. 32, p. 45138, 2017.

[63] C. Mongioví, N. Morin-Crini, V. Placet et al., "Hemp-based materials for applications in wastewater treatment by biosorption-oriented processes: a review," in *Cannabis/Hemp for Sustainable Agriculture and Materials*, D. C. Agrawal, R. Kumar, and M. Dhanasekara, Eds., pp. 239–295, Springer, Singapore, 2022.

[64] G. Crini, "Non-conventional low-cost adsorbents for dye removal: a review," *Bioresource Technology*, vol. 97, no. 9, pp. 1061–1085, 2006.

[65] G. Crini, E. Lichtfouse, L. D. Wilson, and N. Morin-Crini, "Conventional and non-conventional adsorbents for wastewater treatment," *Environmental Chemistry Letters*, vol. 17, no. 1, pp. 195–213, 2019.

[66] G. Crini, "Recent developments in polysaccharide-based materials used as adsorbents in wastewater treatment," *Progress in Polymer Science*, vol. 30, no. 1, pp. 38–70, 2005.

[67] A. Grela, J. Kuc, and T. Bajda, "A review on the application of zeolites and mesoporous silica materials in the removal of non-steroidal anti-inflammatory drugs and antibiotics from water," *Materials*, vol. 14, no. 17, p. 4994, 2021.

[68] R. Petrović, S. Lazarević, I. Janković-Častvan et al., "Removal of trivalent chromium from aqueous solutions by natural clays: valorization of saturated adsorbents as raw materials in ceramic manufacturing," *Applied Clay Science*, vol. 231, p. 106747, 2023.

[69] Y. Zhu, G. Xu, X. Zhang, S. Wang, C. Li, and G. Wang, "Hierarchical porous carbon derived from soybean hulls as a cathode matrix for lithium-sulfur batteries," *Journal of Alloys and Compounds*, vol. 695, pp. 2246–2252, 2017.